ADVANCED MATERIALS
www.advmat.de

Low-Voltage Reversible Electroadhesion of Ionoelastomer Junctions

Hyeong Jun Kim, Lindsay Paquin, Christopher W. Barney, Soonyong So, Baohong Chen, Zhigang Suo, Alfred J. Crosby,* and Ryan C. Hayward**

Electroadhesion provides a simple route to rapidly and reversibly control adhesion using applied electric potentials, offering promise for a variety of applications including haptics and robotics. Current electroadhesives, however, suffer from key limitations associated with the use of high operating voltages (>kV) and corresponding failure due to dielectric breakdown. Here, a new type of electroadhesion based on heterojunctions between ionoelastomer of opposite polarity is demonstrated, which can be operated at potentials as low as ≈1 V. The large electric field developed across the molecular-scale ionic double layer (IDL) when the junction is placed under reverse bias allows for strong adhesion at low voltages. In contrast, under forward bias, the electric field across the IDL is destroyed, substantially lowering the adhesion in a reversible fashion. These ionoelastomer electroadhesives are highly efficient with respect to the force capacity per electrostatic capacitive energy and are robust to defects or damage that typically lead to catastrophic failure of conventional dielectric electroadhesives. The findings provide new fundamental insight into low-voltage electroadhesion and broaden its possible applications.

Reversibly switchable adhesion in response to external stimuli has been of great interest for a wide variety of industrial, biomedical, manufacturing, and robotics applications.[1–3] Among the approaches developed to date, electroadhesion offers simple and reversible control of attractive electrostatic forces between two surfaces subjected to an electric field.[4–6] Compared to other mechanisms, electroadhesion provides several advantages, such as precise control of adhesive force, fast response, lack of residue, quiet operation, and low energy consumption.[7–9] In particular, electroadhesives have become increasingly adopted within the fields of haptics and robotics—for example to enable soft grippers,[10–12] wall climbing robots,[13–15] touchscreens,[16–18] and haptic gloves for touching virtual objects[19,20]—thanks to their ability to function with stretchable dielectrics, small sizes, and low weights.

Current electroadhesives based on electronic conductors and insulating dielectric layers, however, are typically limited by the need for applied potentials in the range of several kV, which, in addition to presenting safety concerns and requiring specialized circuit elements compatible with high voltages,[21] can easily lead to dielectric breakdown and corresponding irreversible device failures.[22,23] One strategy to reduce operating voltage is to decrease the dielectric layer thickness of the electroadhesives, as a standard parallel plate capacitor model would suggest that electrostatic force is inversely proportional to the square of the dielectric thickness.[5,24] Indeed, Chen and Bergbreiter[4] demonstrated that the use of a thin (<0.8 µm) parylene dielectric layer prepared by chemical vapor deposition provided an electroadhesive surface that could support a shear stress of 120 kPa with an operating voltage of only 50 V. Similarly, de Rivaz et al.[13] used a thin (≈12.5 µm) polyimide dielectric layer that supported a 6 kPa shear stress at 250 V. However, reliable fabrication of mechanically robust and defect-free dielectric layers becomes challenging as the thickness of the dielectric layer is further decreased,[4] and operation in the range of only a few volts has not previously been possible with dielectric electroadhesives.

Instead of dielectric layers, charged macromolecules have shown great promise for reversible adhesion operated at substantially lower potentials. Ionic complexation of oppositely charged polyanions and polycations provides reversibly switchable adhesion mechanisms in response to external stimuli, as widely used for adhesion in many biological systems.[25,26] For example, Kobayashi et al.[27] demonstrated reversible adhesion between oppositely charged polyelectrolyte brushes in an aqueous medium. Complex formation between the oppositely charged polyelectrolytes enabled strong adhesion capable of supporting a shear stress of 1.5 MPa, while subsequent addition

Dr. H. J. Kim, L. Paquin, C. W. Barney, Prof. A. J. Crosby, Prof. R. C. Hayward
Polymer Science and Engineering Department
University of Massachusetts
Amherst, MA 01003, USA
E-mail: crosby@mail.pse.umass.edu; hayward@umass.edu
Dr. S. So
Energy Materials Research Center
Korea Research Institute of Chemical Technology
Daejeon 34114, South Korea
B. Chen, Prof. Z. Suo
John A. Paulson School of Engineering and Applied Sciences
Kavli Institute for Bionano Science and Technology
Harvard University
Cambridge, MA 02138, USA
E-mail: suo@seas.harvard.edu
The ORCID identification number(s) for the author(s) of this article can be found under https://doi.org/10.1002/adma.202000600.

DOI: 10.1002/adma.202000600

of salt allowed the two polyelectrolytes to be detached due to the screening of electrostatic interactions. Later, electroswitching of the adhesion between polyanion and polycation hydrogels by creating a concentration gradient of ions using potentials in the range of several volts was demonstrated by Asoh et al.[28] and Morales et al.[29] However, these examples are limited to operation within water, and so far only two adhesion states, either attached or detached, have been achieved. Enabling electroadhesion at low voltages in liquid-free conditions remains an open challenge with significant potential to expand this approach to new applications.

Here, we develop a new class of electroadhesives based on ionoelastomer heterojunctions that can be operated at potentials of ≈1 V. An ionoelastomer is a soft and liquid-free ion conducting network formed by polymerization of an ionic liquid monomer and crosslinker into an elastomer network, such that one ion species is anchored by the network while the other species is mobile.[30–32] We recently established that an "ionic double layer" (IDL) is formed at the interface between two oppositely charged ionoelastomers, analogous to the depletion (or space charge) layer formed at a p/n junction of electronic semiconductors.[30] The voltage drop across the IDL is modulated here to reversibly control the adhesion between two ionoelastomers. Under "reverse bias" as shown in **Figure 1**A, the mobile ions are pulled away from the interfacial region, leading to a build-up of excess fixed charges in the IDL. The electric field generated by these excess fixed charges in the thin interfacial layer induces electrostatic adhesion between the two ionoelastomers. Under "forward bias" (Figure 1B), mobile cations are driven from the polyanion domain into the polycation domain, and vice versa for mobile anions. Thus, the interface behaves resistively and the electrostatic adhesion between the two ionoelastomers is lost (see Video S1 in the Supporting Information).

We demonstrate ionoelastomer-based electroadhesion using crosslinked networks of 1-ethyl-3-methyl imidazolium poly[(3-sulfopropyl) acrylate] (ES) and poly[1-(2-acryloyloxyethyl)-3-buthylimidazolium]bis(trifluoromethane) sulfonimide (AT) (Figure S1, Supporting Information).[30] Highly crosslinked ES and AT (containing 20 mol% of poly(ethylene glycol) diacrylate crosslinker) are used to reduce the adhesion between the two ionoelastomers in the absence of an applied voltage, and both ionoelastomers are reinforced by adding fumed silica particles (2.5 wt%). To maximize the voltage drop across the IDL at the ES/AT junction, we embed microporous layer (MPL) carbon electrodes within each layer, on the side distal to the junction. The high surface area of the MPL electrodes provides roughly a 10^3-fold larger capacitance ($\approx 10^{-3}$ F cm^{-2}) of the electrical double layer (EDL) formed at the ionoelastomer/electrode interface compared to that of the IDL ($\approx 10^{-6}$ F cm^{-2}) formed at the planar ES/AT interface, as measured by AC impedance following our previous report.[30] Details on the fitting parameters, including ionic conductivities of the ionoelastomer layers, are shown in Tables S1–S4 (Supporting Information). Due to the several order-of-magnitude difference in the capacitance of the EDLs and the IDL, the applied voltage is dropped almost entirely across the smallest capacitor, i.e., the IDL, and can most effectively be used for electroadhesion.

To characterize the electroadhesion between ES and AT ionoelastomers, we use a contact adhesion test with a crossed-cylinder geometry[33–35] (**Figure 2**A). According to the Derjaguin approximation, crossed cylinders are equivalent to a sphere-on-flat geometry, which will generate a well-defined point of contact and minimize the effects of air gaps on electroadhesion.[35] In practice, additional design factors would be implemented to minimize air gaps due to geometric irregularities (e.g., roughness) on relevant size scale.[36–38] The applied load (P) and displacement (δ) are measured (Figure 2B) as the two perpendicularly crossed cylinders (with radius r = 10 mm; Figure S4, Supporting Information) are brought together to generate contact between ES and AT layers at a constant speed of 0.05 mm s^{-1}, held at fixed displacement for 30 s to charge the ionoelastomers, and then separated with the same speed of 0.05 mm s^{-1} at fixed voltage (Figure S5, Supporting Information). To measure the electrostatic force under steady-state conditions, we apply 30 s of charging time (Figure S6, Supporting Information), which is longer than the RC timescale for charging of the IDL ($\tau_{RC} \approx 60$ ms) as well as the timescale for

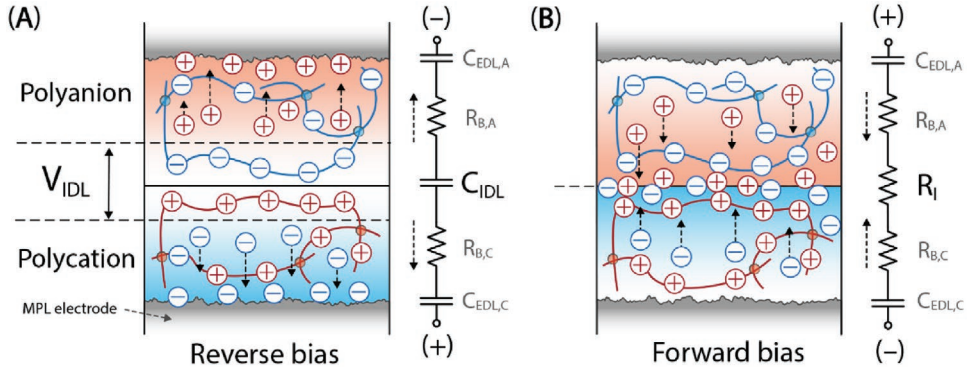

Figure 1. A,B) Schematic illustrations of a polyanion/polycation ionoelastomer junction operated under reverse bias (A) and forward bias (B). Under reverse bias, where the polyanion is connected to the negative terminal and the polycation is connected to the positive terminal of the power supply, the voltage drop (V_{IDL}) across the ionic double layer (IDL) provides electrostatic adhesion between the two ionoelastomers. In contrast, under forward bias, mobile ions meet at the interface, destroying the electric field in the IDL and thereby dramatically lowering the adhesion. $R_{B,A}$ and $R_{B,C}$ correspond to the bulk resistance of the polyanion and polycation, respectively. $C_{EDL,A}$ and $C_{EDL,C}$ correspond to the capacitance of the electric double layer (EDL) formed at the interface of the electrode/polyanion and the electrode/polycation, respectively, while C_{IDL} corresponds to the capacitance of the IDL.

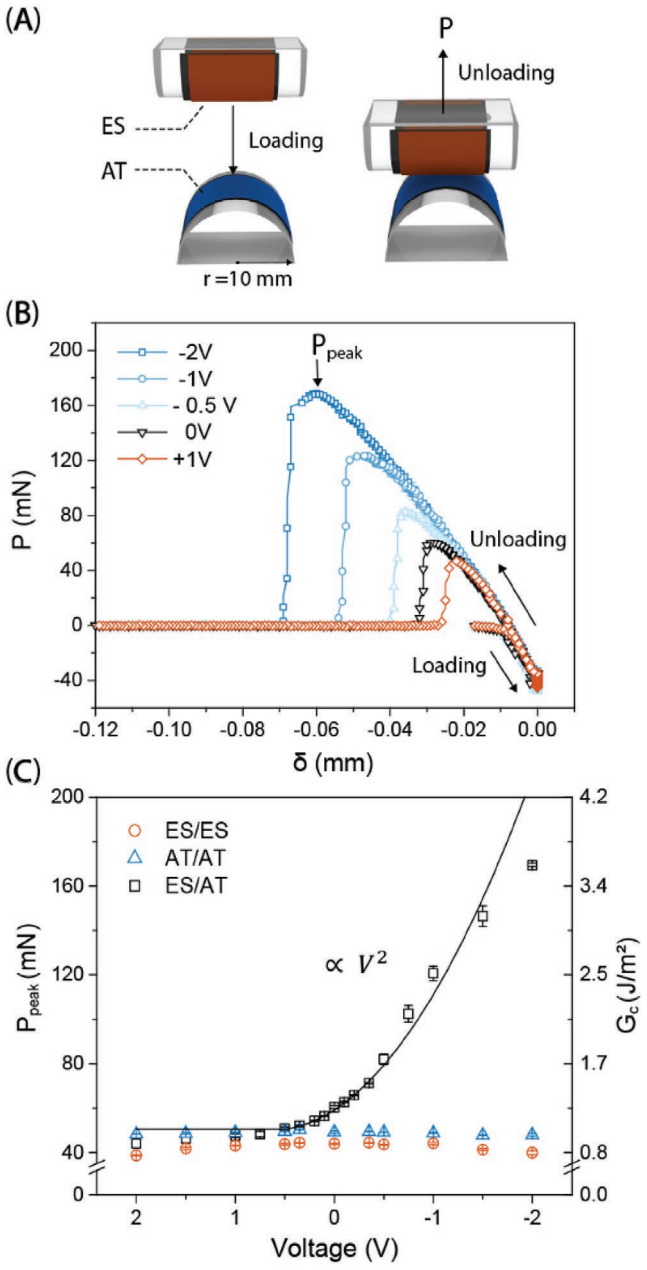

Figure 2. A) A schematic illustration of the contact adhesion test using a crossed-cylinder geometry. B) Representative load–displacement curves from the ES/AT junction under external biases where the blue and red data points represent reverse and forward bias, respectively. C) Values of P_{peak} for the three ionoelastomer junctions, i.e., ES/ES and AT/AT homo-junctions and ES/AT heterojunction. The ES/AT heterojunction shows a quadratic increase of P_{peak} as a function of voltage. The black line represents a fit to $P_{peak} = A(V_B - V)^2 + P_0$ for $V \leq V_B$, where $A = 28 \pm 1$ mN V^{-2}, $V_B = 0.5 \pm 0.1$ V, and $P_0 = 50 \pm 3$ mN.

stress relaxation of the contact force (see the Supporting Information for details). According to the Johnson–Kendal–Roberts (JKR) model for adhesive contact between elastic materials, the peak separation load (P_{peak}) can be translated into a critical strain energy release rate (G_c) by $P_{peak} = (3/2)\pi r G_c$.[39] Figure 2C shows the values of P_{peak} and G_c for three ionoelastomer junctions, i.e., ES/ES and AT/AT homo-junctions, and an ES/AT hetero-junction, under various applied voltages. Additional data for an ES/AT hetero-junction with a shorter charging time of 1 s is shown in Figure S7 (Supporting Information). Both the ES/ES and AT/AT homo-junctions are insensitive to voltage, showing respective P_{peak} values of 42 ± 2 and 48 ± 3 mN, corresponding to G_c of 0.9 ± 0.1 and 1.0 ± 0.1 J m^{-2}. In contrast, the ES/AT heterojunction shows a dramatic increase in P_{peak} and G_c as a function of voltage. When a forward bias exceeding the built-in voltage of the ES/AT junction ($V \geq 0.5$ V) is applied, drift of mobile ions destroys the IDL at the interface. Then, a constant P_{peak} of 50 ± 3 mN and G_c of 1.1 ± 0.1 J m^{-2} are measured, similar to that of the homo-junctions, suggesting that this is characteristic of the background adhesion level between ES and AT ionoelastomers without electroadhesion. In contrast, when a reverse bias is applied, charging the IDL capacitor leads to a quadratic increase of P_{peak} and G_c with voltage, as expected for the electrostatic force.[4,13,19] For example, under a reverse bias of –2 V applied to the ES/AT junction, P_{peak} is measured to be 170 ± 2 mN, and G_c is increased to 3.6 ± 0.1 J m$^{-2,}$ which are roughly 4-times larger than the values at or above +0.5 V. We anticipate that substantial improvements in the on/off ratio of adhesive force should be possible by reducing the background adhesion level through suitable modifications to the polymers, e.g., by substantially reducing their glass transition temperatures, as well as by modifying the geometry of the adhesive device.[40]

For a deeper understanding of the adhesion and elasticity of ES/AT ionoelastomers, we directly measure the contact area between two ionoelastomers during the contact adhesion test using a custom-built contact adhesion apparatus on an optical microscope (full details in in the Supporting Information). Since the MPL carbon electrodes are not optically transparent, we use bare ES and AT ionoelastomers without electrodes to measure the contact area (Movie S2, Supporting Information). In this case, P_{peak} of ES/AT is measured to be 59 ± 2 mN, consistent with the value at an applied potential of 0 V in Figure 2 ($P_{peak} = 61 \pm 1$ mN), and the contact area at peak force is observed to be 0.31 ± 0.02 mm^2 (Figure S8, Supporting Information). Then, measured load, displacement and contact radius during the test are analyzed using the JKR model with axial confinement and interfacial friction corrections,[33] as described in detail in the Supporting Information. The plane strain modulus (E^*) of ES/AT extracted from the JKR model is 2.3 ± 0.4 MPa. In the adhesive contact region during unloading, G_c is calculated to be 1.8 ± 0.2 J m^{-2}, which is similar to the value of $G_c = 1.3 \pm 0.1$ J m^{-2} at 0 V estimated previously from the relationship $P_{peak} = (3/2)\pi r G_c$.

The reversibility of ES/AT electroadhesives is tested by measuring P_{peak} multiple times under an alternating voltage of ± 1 V. During 30 repeated cycles, consistent values of P_{peak} = 106 ± 5 mN for the "on"-state (–1 V) and 41 ± 4 mN for the "off"-state (+1 V) are observed (**Figure 3**A). The corresponding values of G_c for the on- and off-states are 2.3 and 0.9 J m^{-2}, respectively. In addition, we further measure G_c for the peeling of ES and AT as shown in the inset of Figure 3B following previously described methods.[3] At a crack speed of 0.2 mm s^{-1}, the two ionoelastomers peel easily at +1 V, yielding $G_c = 82 \pm 6$ J m^{-2}. In contrast, at –1 V, a substantially higher value of $G_c = 220 \pm 3$ J m^{-2} is

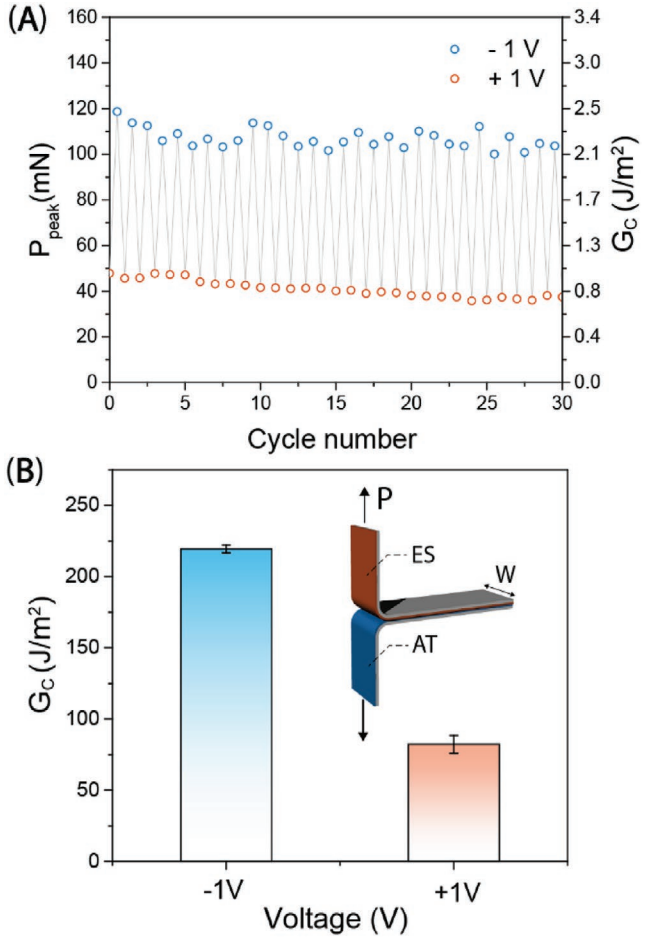

Figure 3. A) P_{peak} of ES/AT heterojunctions measured by contact adhesion tests under an alternating voltage of ±1 V. The blue dots represent reverse bias (−1 V) and the red dots represent forward bias (+1 V). B) T-peel test of ES/AT heterojunctions for measuring the energy release rate for peeling (G_c).

measured. We expect that the larger value of G_c compared to that of the contact adhesion tests is predominantly an effect of the relatively fast crack propagation speed during the T-peel test. Critically, the electroadhesion between ES and AT layers is much more robust to defects compared to conventional electroadhesives. As an example, we scratch the surfaces of electroadhesives with a scalpel (see Video S3 in the Supporting Information). While the electroadhesive properties of the ionoelastomer junction are maintained after damaging the surfaces, a conventional dielectric electroadhesive shows dielectric failure and a complete loss of electroadhesion when subjected to the same conditions.

We next consider the mechanism of reversible electroadhesion of ES and AT ionoelastomers in more detail. When the ES/AT electroadhesive is operated under reverse bias, additional mobile ions are pulled away from the interface, leading to a build-up of excess voltage in the IDL. This depleted zone of mobile ions of characteristic thickness δ surrounding the interface will experience an electrostatic force (F_e) with a magnitude of $F_e = 1/2\varepsilon_0\varepsilon_r A(V_B - V)^2/\delta^2$, where V_B is the built-in potential of the ES/AT junction, A is the contact area, and ε_0 and ε_r are the vacuum and relative dielectric permittivity, respectively. Based on the Gouy–Chapman model,[41] the specific capacitance of the double layer is $C \approx \varepsilon_0\varepsilon_r/\delta$ for small V, and we measure the IDL capacitance to be $C_{IDL} \approx 1$ μF cm^{-2} by AC impedance (Table S4, Supporting Information). Therefore, from the coefficient of quadratic fitting in Figure 2C ($1/2\varepsilon_0\varepsilon_r A/\delta^2 \approx 1/2C_{IDL}A/\delta = 28 \pm 1$ mN V^{-2}) and the measured contact area ($A = 0.31 \pm 0.02$ mm^2) at 0 V, we can estimate δ to be ≈50 nm.

An ionoelastomer junction provides higher force capacity at equivalent stored electrostatic energy ($E = 1/2CV^2$) compared to other dielectric systems, since the electrostatic force is developed over a very thin interfacial layer δ and the force capacity per unit energy ratio scales as the inverse of the characteristic thickness at a constant voltage.[24] The force capacity per unit energy of an ES/AT junction at −1 V is found here to be 4.2×10^4 kN J^{-1} while other dielectric electroadhesives show substantially smaller values, e.g., 1.2 kN J^{-1} for 12.5 μm thick polyimide at 1 kV,[19] 62 kN J^{-1} for 9 μm thick silicone at 200 V,[13] and 1.1×10^3 kN J^{-1} for 0.8 μm thick parylene at 50 V.[4] Moreover, the capacitance of the IDL (≈10^{-6} F cm^{-2}) is much larger than that of typical dielectric capacitors (≈10^{-9} to 10^{-12} F cm^{-2}),[13,42,43] which allows a large amount of electrostatic energy to be stored in the capacitor at low voltages. The electrical energy consumption by ES/AT ionoelastomer adhesives at −1 V during the contact adhesion test is 10.6 ± 1.0 μJ (Figure S12A, Supporting Information). In comparison, the additional mechanical work required to break the adhesive contact at −1 V, compared to 0 V, is estimated as 0.39 ± 0.03 μJ, corresponding to 4% of the electrical energy input. The dominant source of energy loss is a leakage current across the IDL interface, and thus with a shorter charging time of 1 s (Figure S12B, Supporting Information) this value can be increased to 15%. Further refinements to the material system to reduce the concentration of residual monomer impurities and/or to increase the interfacial resistance, and thereby to reduce the leakage current, should enable additional improvements in this performance metric in the future. Details are provided in the Supporting Information.

Further evidence for this picture of ionoelastomer electroadhesion is provided by AC-impedance measurements of ES/AT junctions under applied DC biases (**Figure 4**), as described using the previously developed equivalent circuit model shown in the inset of Figure 4A.[30] In brief, this model contains a dielectric capacitance (C_B) corresponding to the polarization of the ionoelastomer at high frequency, and three resistors corresponding to the drift of free ions (R_B), the interfacial ionic current (R_I), and the contact resistance (R_C). A constant phase element (CPE) is used to describe the double layer capacitors, i.e., the EDL at the electrode/ionoelastomer interface (CPE_{EDL}) and the IDL at the ES/AT interface (CPE_{IDL}). When a reverse bias is applied, the interfacial resistance (R_I) increases significantly (Table S4, Supporting Information), leading to a high impedance in the low AC frequency regime (<100 Hz) (blue lines in Figure 4) and thereby charging the IDL, as described by the constant phase element (CPE_{IDL}) in the circuit model. Note that the effective capacitance of the IDL is much smaller than that of the EDLs due to the high surface area of the MPL electrodes, and thus the voltage drop occurs almost entirely across the IDL. Under forward bias, mobile ions meet at the interface to generate a non-Faradaic ionic current, resulting in a small R_I. This leads to a decrease of the electric field at the interface as the IDL is destroyed, as clearly revealed by the dramatic decrease

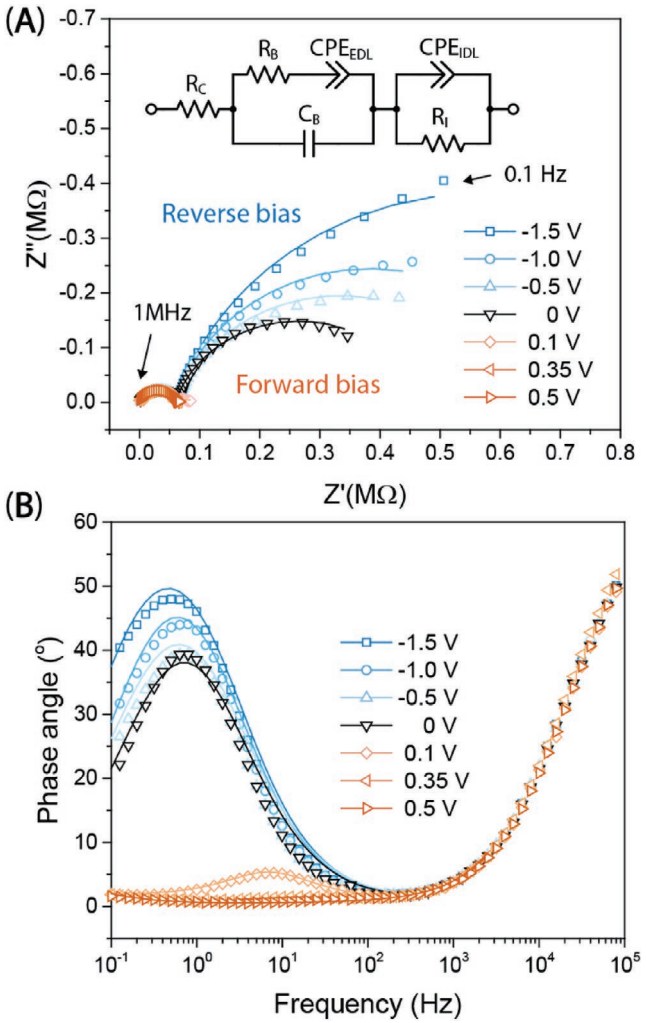

Figure 4. A,B) AC-impedance measurements shown as Nyquist plots (A) and Bode phase plots (B) for ES/AT heterojunctions under the DC biases indicated in the legend. The blue and red colors represent reverse and forward biases, respectively. The solid lines represent fits of the equivalent circuit model shown in the inset of (A).

in the low-frequency peak in phase angle from 0.01 to 100 Hz (Figure 4B).

Finally, we demonstrate an ionoelastomer electroadhesive pad that can withstand a shear load of 5 kPa at +1 V, as shown in **Figure 5**. This pad consists of two counterparts: one contains ES and AT connected to the power source, while the other contains the two ionoelastomers connected by a conductive wire. With this geometry, the second pad can be used for holding a weight without being connected to the power supply. A circuit diagram of this system is shown in the inset of Figure 5A. When –1 V is applied to the ionoelastomer electroadhesion pads—each of which contains 1 cm^2 of ES and AT—they can hold a weight of 100 g, corresponding to a shear stress of 5 kPa. When the external voltage is switched to +1 V, the pads lose adhesion and detach from each other within a time scale of ≈1 s (see Video S4 in the Supporting Information). We expect that these ionoelastomer junction electroadhesives will be particularly attractive for the design of soft and microrobotic applications as they can

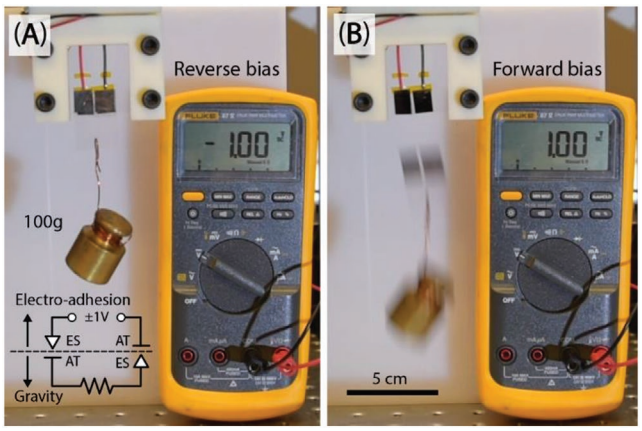

Figure 5. ES/AT ionoelastomer electroadhesion pads capable of withstanding a 5 kPa shear load at an applied potential of –1 V. These pads consist of two counterparts: one contains ES and AT layers connected to the power source, while the other contains ES and AT layers connected with a conductive wire. The operation is shown in Video S4 (Supporting Information).

be controlled without the need for large and heavy high-voltage amplifiers or specially designed high voltage operable transistors and logic elements. We note that in the current implementation, ionoelastomer electroadhesives provide enhanced adhesion only between two specific materials of opposite polarity. While such selective complementary adhesion can be useful in its own right (e.g., Velcro, zippers, and buttons),[44] it would also be valuable to achieve low-voltage adhesion to a greater variety of other surfaces using ionoelastomers. To this end, we are currently pursuing approaches to laterally pattern high surface area electrodes and alternating domains of ionoelastomers of opposite polarity as an analog to the interdigitated structures commonly employed to enable versatile adhesion of dielectric electroadhesives to different types of materials.[9,45]

In conclusion, we have demonstrated that an ionoelastomer junction provides a new type of electroadhesive that can be controlled with low voltages (≈1 V). Under reverse bias, charging the interfacial ionic double layer provides an electrostatic force between the two ionoelastomers, while under forward bias mobile ions are pushed into the IDL and ultimately across the interface, destroying the electric field and thereby substantially lowering the adhesion. Therefore, our findings offer a fundamentally new platform for designing electroadhesives capable of reversibly switchable adhesion at low operating voltages, and which are far more tolerant to damage than conventional dielectric electroadhesives. As an example, we demonstrate ionoelastomer electroadhesive pads that can reversibly switch on and off at potentials of ±1 V, and are capable of supporting a shear stress of 5 kPa. We expect that this approach will open new opportunities in numerous areas, including robotics, virtual reality hardware, and responsive materials.

Experimental Section

Preparation of ES and AT Ionoelastomers: The monomers for ES and AT were synthesized following the previous work.[30] Two-step free radical polymerization reactions were used to prepare ES and AT ionoelastomers

on MPL electrodes. During the first step, ES (or AT) monomer (1 g) was vigorously mixed with 20 mol% of poly(ethylene glycol) diacrylate (PEGDA, average molecular weight 250 g mol^{-1}, Sigma-Aldrich) and 0.5 mol% of azobisisobutyronitrile (AIBN, recrystallized, Sigma-Aldrich) solution in ethanol (10 mg mL^{-1}). After mixing, 0.1 g of this solution was diluted with 500 µL of ethanol and drop-cast onto a 2.5 cm x 4 cm piece of MPL electrode (29BC, Sigracet). The ethanol was allowed to evaporate for 12 h at room temperature before the sample was placed into a glass chamber and polymerized under N_2 in a 60 °C oven overnight. This allows ES and AT monomers to fully infiltrate the MPL electrode. After this first step, the remaining ES (or AT) solution was mixed with 2.5 wt% of fumed silica (CAB-O-SIL TS530, Cabot) to enhance the fracture toughness of the resulting ionoelastomers. The fumed silica was dissolved in ethanol with a concentration of 10 wt% and sonicated for 3 h before use. The coated MPL electrode was placed between two fluorinated glass slides separated by 250 µm poly(tetrafluoroethylene) (PTFE) spacers. Then, the monomer solution was injected into this mold, followed by polymerization under N_2 in a 60 °C oven overnight. Unreacted monomers were extracted by washing with isopropanol several times, and the ionoelastomer layers were dried at 60 °C in a vacuum oven to remove residual solvents and water before use.

Contact Adhesion Test: A commercial tensile testing system (TA.TX plus texture analyzer, StableMicrosystems) was used to measure the load (P) and displacement (δ) during the contact adhesion test. Custom-designed cylinder fixtures (Figure S4, Supporting Information) were produced using a 3D printer (uPrint SE Plus, Stratasys), where the radius of the cylinder was 10 mm. An ES (or AT) elastomer film on an MPL electrode was cut into a rectangular shape (5 mm × 40 mm) and placed on top of a fixture. Two cylinder fixtures covered with ionoelastomers were then connected to the tensile testing system. The two cylinders were translated toward each other at a constant speed of 0.05 mm s^{-1} until the load reached 50 mN. Then, the ionoelastomers were connected to an external voltage source set to the desired potential. After a dwell time of 30 s, the two cylinders were separated at 0.05 mm s^{-1} while the load and displacement were recorded.

T-Peel Test: The T-peel test was used to measure the energy release rate G_c for peeling of ES and AT junctions (Figure 3B, inset). Ionoelastomer samples containing MPL electrodes were prepared with dimensions of 10 mm in width W and 45 mm in length. The backsides of each were glued to a stiff polycarbonate film (125 µm thickness) using an epoxy adhesive (Loctite EA 9017, Henkel-Adhesives). The ES and AT layers were attached to each other, while their free ends were affixed to the tensile testing system. The ES and AT layers were connected to the external power source to maintain the desired potential, while peeling was conducted by separating the two ionoelastomers at a fixed rate of 0.2 mm s^{-1}. The value of G_c was calculated as $G_c = 2P_a/W$, where P_a is the average load during peeling.

AC-Impedance Measurement: AC-impedance measurements of ionoelastomer junctions were conducted using a Reference 600^+ instrument (Gamry Instruments) with AC amplitude of 40 mV over a frequency range of 1 MHz to 0.1 Hz. Two probes were used, with the positive terminal (working electrode) connected to ES and negative terminal (counter and reference electrodes) connected to AT. Experimental AC impedance data were fitted using ZView software (Scribner Associates). Details of the fits are described in the Supporting Information.

Supporting Information

Supporting Information is available from the Wiley Online Library or from the author.

Acknowledgements

This work was supported by the National Science Foundation under Grant No. DMR-1609972. C.B. was funded by the Office of Naval Research (ONR N00014-17-1-2056), and A.J.C's work was funded by the U.S. Army Research Laboratory and the U.S. Army Research Office under Contract/Grant No. W911NF-15-1-0358.

Conflict of Interest

The authors declare no conflict of interest.

Keywords

contact mechanics, electroadhesion, ionic double layer, ionoelastomer junction, ionotronics

Received: January 27, 2020
Revised: April 17, 2020
Published online:

[1] M. Kamperman, A. Synytska, *J. Mater. Chem.* **2012**, *22*, 19390.
[2] M. Liu, L. Jiang, *Adv. Funct. Mater.* **2010**, *20*, 3753.
[3] Y. Gao, K. Wu, Z. Suo, *Adv. Mater.* **2019**, *31*, 1806948.
[4] A. S. Chen, S. Bergbreiter, *Smart Mater. Struct.* **2017**, *26*, 025028.
[5] K. H. Koh, R. M. K. Chetty, S. G. Ponnambalam, presented at *2011 IEEE ROBIO*, Karon Beach, Phuket, Thailand, December **2011**.
[6] M. Taghavi, T. Helps, J. Rossiter, *Sci. Rob.* **2018**, *3*, eaau9795.
[7] J. Germann, B. Schubert, D. Floreano, presented at *2014 IEEE/RSJ IROS*, Chicago, IL, USA, September **2014**.
[8] H. Prahlad, R. Pelrine, S. Stanford, J. Marlow, R. Kornbluh, presented at *2008 IEEE ICRA*, Pasadena, CA, USA, May **2008**.
[9] J. Guo, T. Bamber, M. Chamberlain, L. Justham, M. Jackson, *J. Phys. D: Appl. Phys.* **2016**, *49*, 415304.
[10] J. Shintake, S. Rosset, B. Schubert, D. Floreano, H. Shea, *Adv. Mater.* **2016**, *28*, 231.
[11] V. Cacucciolo, J. Shintake, H. Shea, presented at *2019 2nd IEEE Int. Conf. on Soft Robotics*, Seoul, Korea, April **2019**.
[12] J. Shintake, V. Cacucciolo, D. Floreano, H. Shea, *Adv. Mater.* **2018**, *30*, 1707035.
[13] S. D. de Rivaz, B. Goldberg, N. Doshi, K. Jayaram, J. Zhou, R. J. Wood, *Sci. Rob.* **2018**, *3*, eaau3038.
[14] G. Gu, J. Zou, R. Zhao, X. Zhao, X. Zhu, *Sci. Rob.* **2018**, *3*, eaat2874.
[15] J. Guo, J. Leng, J. Rossiter, *IEEE Trans. Rob.* **2020**, *36*, 313.
[16] M. Ayyildiz, M. Scaraggi, O. Sirin, C. Basdogan, B. N. J. Persson, *Proc. Natl. Acad. Sci. USA* **2018**, *115*, 12668.
[17] O. Sirin, M. Ayyildiz, B. N. J. Persson, C. Basdogan, *Soft Matter* **2019**, *15*, 1758.
[18] X. Li, C. Choi, Y. Ma, P. Boonpuek, J. R. Felts, J. Mullenbach, C. Shultz, J. E. Colgate, M. C. Hipwell, *IEEE Trans. Haptics* **2020**, *13*, 1.
[19] R. Hinchet, V. Vechev, H. Shea, O. Hilliges, presented at *31st Annu. ACM Sympo. on UIST*, Berlin, Germany, October **2018**.
[20] R. Hinchet, H. Shea, *Adv. Mater. Technol.* **2020**, *5*, 1900895.
[21] A. Marette, A. Poulin, N. Besse, S. Rosset, D. Briand, H. Shea, *Adv. Mater.* **2017**, *29*, 1700880.
[22] J. P. D. Téllez, J. Krahn, C. Menon, presented at *2011 IEEE ROBIO*, Karon Beach, Phuket, Thailand, December **2011**.
[23] M. Ghilardi, J. J. C. Busfield, F. Carpi, presented at *Electroactive Polymer Actuators and Devices (EAPAD)*, OR, USA, April **2017**.
[24] K. H. Koh, M. Sreekumar, S. G. Ponnambalam, *Materials* **2014**, *7*, 4963.
[25] Q. Zhao, D. W. Lee, B. K. Ahn, S. Seo, Y. Kaufman, Jacob N. Israelachvili, J. H. Waite, *Nat. Mater.* **2016**, *15*, 407.

[26] C. G. de Kruif, F. Weinbreck, R. de Vries, *Curr. Opin. Colloid Interface Sci.* **2004**, *9*, 340.
[27] M. Kobayashi, M. Terada, A. Takahara, *Soft Matter* **2011**, *7*, 5717.
[28] T.-A. Asoh, W. Kawai, A. Kikuchi, *Soft Matter* **2012**, *8*, 1923.
[29] D. Morales, E. Palleau, M. D. Dickey, O. D. Velev, *Soft Matter* **2014**, *10*, 1337.
[30] H. J. Kim, B. Chen, Z. Suo, R. C. Hayward, *Science* **2020**, *367*, 773.
[31] A. S. Shaplov, P. S. Vlasov, E. I. Lozinskaya, D. O. Ponkratov, I. A. Malyshkina, F. Vidal, O. V. Okatova, G. M. Pavlov, C. Wandrey, A. Bhide, M. Schönhoff, Y. S. Vygodskii, *Macromolecules* **2011**, *44*, 9792.
[32] J.-H. Choi, W. Xie, Y. Gu, C. D. Frisbie, T. P. Lodge, *ACS Appl. Mater. Interfaces* **2015**, *7*, 7294.
[33] K. R. Shull, D. Ahn, W.-L. Chen, C. M. Flanigan, A. J. Crosby, *Macromol. Chem. Phys.* **1998**, *199*, 489.
[34] K. R. Shull, *Mater. Sci. Eng., R* **2002**, *36*, 1.
[35] A. Falsafi, M. Tirrell, A. V. Pocius, *Langmuir* **2000**, *16*, 1816.
[36] B. N. J. Persson, J. Guo, *Soft Matter* **2019**, *15*, 8032.
[37] M. D. Bartlett, A. B. Croll, D. R. King, B. M. Paret, D. J. Irschick, A. J. Crosby, *Adv. Mater.* **2012**, *24*, 1078.
[38] D. R. King, M. D. Bartlett, C. A. Gilman, D. J. Irschick, A. J. Crosby, *Adv. Mater.* **2014**, *26*, 4345.
[39] D. Maugis, M. Barquins, *J. Phys. D: Appl. Phys.* **1978**, *11*, 1989.
[40] E. P. Chan, C. Greiner, E. Arzt, A. J. Crosby, *MRS Bull.* **2007**, *32*, 496.
[41] M. Muthukumar, *Polymer Translocation*, CRC Press, Boca Raton, FL, USA **2016**.
[42] S. C. B. Mannsfeld, B. C. K. Tee, R. M. Stoltenberg, C. V. H. H. Chen, S. Barman, B. V. O. Muir, A. N. Sokolov, C. Reese, Z. Bao, *Nat. Mater.* **2010**, *9*, 859.
[43] J.-Y. Sun, C. Keplinger, G. M. Whitesides, Z. Suo, *Adv. Mater.* **2014**, *26*, 7608.
[44] D. R. King, M. D. Bartlett, M. Nalbach, D. J. Irschick, A. J. Crosby, *J. Polym. Sci., Part B: Polym. Phys.* **2017**, *55*, 1783.
[45] N. Berdozzi, Y. Chen, L. Luzi, M. Fontana, I. Fassi, L. M. Tosatti, R. Vertechy, *IEEE Rob. Autom. Lett.* **2020**, *5*, 2770.